Trapping of Hepatitis B Virus Capsid Assembly Intermediates by Phenylpropenamide Assembly Accelerators

Sarah P. Katen[†], Srinivas Reddy Chirapu[‡], M. G. Finn[‡], and Adam Zlotnick[†],*

[†]Department of Biochemistry, Indiana University, Bloomington, Indiana 47405, United States and [‡]Department of Chemistry and The Skaggs Institute for Chemical Biology, The Scripps Research Institute, 10550 N. Torrey Pines Rd., La Jolla, California 92037, United States

Virus capsid assembly is an exquisitely choreographed process in which hundreds of viral and host components come together with high fidelity to form a viable virus particle (*1*). In the case of the hepatitis B virus (HBV), an icosahedral DNA virus with an RNA intermediate, assembly involves the concerted association of 120 dimeric capsid subunits (core protein homodimers) to form a $T = 4$ icosahedron, which packages the RNA form of the 3.5 kb viral genome, the viral reverse transcriptase (Pol), and assorted host proteins (*2–4*). The HBV core plays a central role in the virus life cycle, participating in genome packaging, reverse transcription, intracellular trafficking, and maintenance of a stable infection (*5–7*). The HBV assembly process depends on the coordinated interactions of many components, providing many opportunities for missteps and yet proceeding with remarkable success.

Like many icosahedral viruses, the capsid of HBV spontaneously self-assembles from many copies of a single protein (*8*). Capsid assembly can be modeled as a variation of a polymerization reaction. For capsids, spherical polymers of defined size, the lag phase corresponds to the formation of nuclei and accumulation of an assembly line of intermediates. During the exponential phase, complete capsids appear while free subunits are consumed to replenish the intermediates, entering a steady state. As assembly plateaus, the concentration of intermediates remains constant (though undetectably low), and the rate of formation of capsids is equal to the rate of formation of new nuclei. To minimize kinetic trapping and allow for repair of errors, subunits interact through weak individual contact energies (*9, 10*). Icosahedral viruses maintain their structure through the

ABSTRACT Understanding the biological self-assembly process of virus capsids is key to understanding the viral life cycle, as well as serving as a platform for the design of assembly-based antiviral drugs. Here we identify and characterize the phenylpropenamide family of small molecules, known to have antiviral activity *in vivo*, as assembly effectors of the hepatitis B virus (HBV) capsid. We have found two representative phenylpropenamides to be assembly accelerators, increasing the rate of assembly with only modest increases in the stability of the HBV capsids; these data provide a physical-chemical basis for their antiviral activity. Unlike previously described HBV assembly effectors, the phenylpropenamides do not misdirect assembly; rather, the accelerated reactions proceed on-path to produce morphologically normal capsids. However, capsid assembly in the presence of phenylpropenamides is characterized by kinetic trapping of assembly intermediates. These traps resolve under conditions close to physiological, but we found that trapped intermediates persist under conditions that favor phenylpropenamide binding and strong core protein−protein interactions. The phenylpropenamides serve as chemical probes of the HBV capsid assembly pathway by trapping on-path assembly intermediates, illustrating the governing influence of reaction kinetics on capsid assembly.

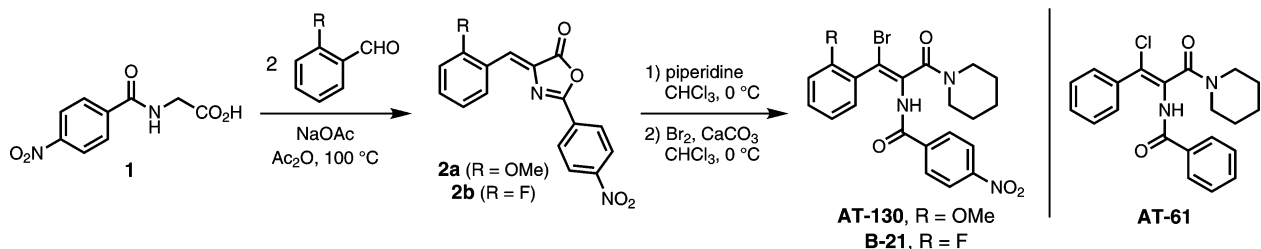*Corresponding author,
azlotnic@indiana.edu.

Figure 1. Phenylpropenamide synthesis pathway and structures.

inherent stability of their geometry because subunits are multivalent. Thus, capsid assembly mimics a two-state reaction with only assembly units and capsids, except where kinetically trapped intermediates accumulate (*11, 12*). Nonetheless, assembly must involve many intermediates resulting in numerous assembly paths that can reflect local environment (*13–17*). Given the quasi-equivalence of the capsid, there is no way to predict or direct the sequence of the degenerate elongation steps that form a capsid (*14, 15*). A means to chemically halt or disrupt these normal assembly processes would provide a unique window into the capsid assembly reaction.

In vitro HBV assembly matches well with theoretical predictions (*18*). The rate-limiting step of the HBV capsid assembly reaction is the slow formation of nuclei, a trimer of core protein dimers (*18*). Assembly of empty capsids is recapitulated by assembly on RNA, which also shows two-state behavior, though with a much lower apparent dissociation constant (*19*). *In vivo*, the HBV assembly process is probably allosterically regulated, so that assembly is initiated only by binding to correct host partners or viral components, thus ensuring packaging of the correct cargo at the correct time (*10, 20, 21*). Thus, altering the conformational state of the core protein can result in a slight increase in the pairwise contact energies or the rate of nucleation and can effectively deregulate capsid assembly. For example, induction of HBV assembly *in vitro* by high concentrations of zinc causes kinetic trapping of the assembly reaction due to overnucleation so that the free subunit pool is depleted before capsids are completed, resulting in the accumulation of fragments (*12*). In extreme cases, perturbation of the interactions of the core protein can misdirect assembly from the normal pathways to form noncapsid polymers. This effect has been achieved chemically with the heteroaryldihydropyrimidine (HAP) small molecule effectors, which increase the

rate and extent of the assembly reaction, and can misdirect the HBV core protein to form large pleomorphic structures (*22–26*). Low concentrations of HAP are not sufficient to misdirect assembly; however, their antiviral effects and replication inhibition can be correlated to the extent to which they alter the rate of assembly (*23*). Clearly, even slight alterations in the reaction can severely impair normal virus assembly.

Molecules of the phenylpropenamide family of compounds were initially identified as specific inhibitors of HBV production in cell culture (*27*). The derivative AT-61 (Figure 1) was first found to inhibit production of both wildtype and lamivudine-resistant HBV. A second derivative, AT-130 (Figure 1), was found to have an even more potent inhibiting activity against both wildtype and reverse-transcriptase inhibitor-resistant strains in culture. A decrease in RNA-containing cores upon treatment with AT-61 led to the hypothesis that the phenylpropenamide compounds affect assembly on the level of RNA packaging (*28*). Subsequent studies conducted with AT-130 have shown that the phenylpropenamides do not effect HBV RNA production, viral protein translation, Pol activity, or core morphology, but do result in the production of empty capsids (*29, 30*).

Here we show that the phenylpropenamides are effectors of HBV capsid assembly and can serve as chemical probes to further our understanding of the mechanism and pathway of HBV capsid assembly. We demonstrate that the compound AT-130 and the fluorinated derivative B-21 (Figure 1) increase both the rate and extent of capsid assembly *in vitro*. The phenylpropenamides appear to bind to the core protein with weak affinity and induce the protein into a more assembly-active state. This increase in the concentration of dimer in the active conformation results in an increased nucleation rate, driving capsid assembly forward. In the case of B-21, this results in reversible kinetic trapping, which can stall the assembly reaction as a mix of intermedi-
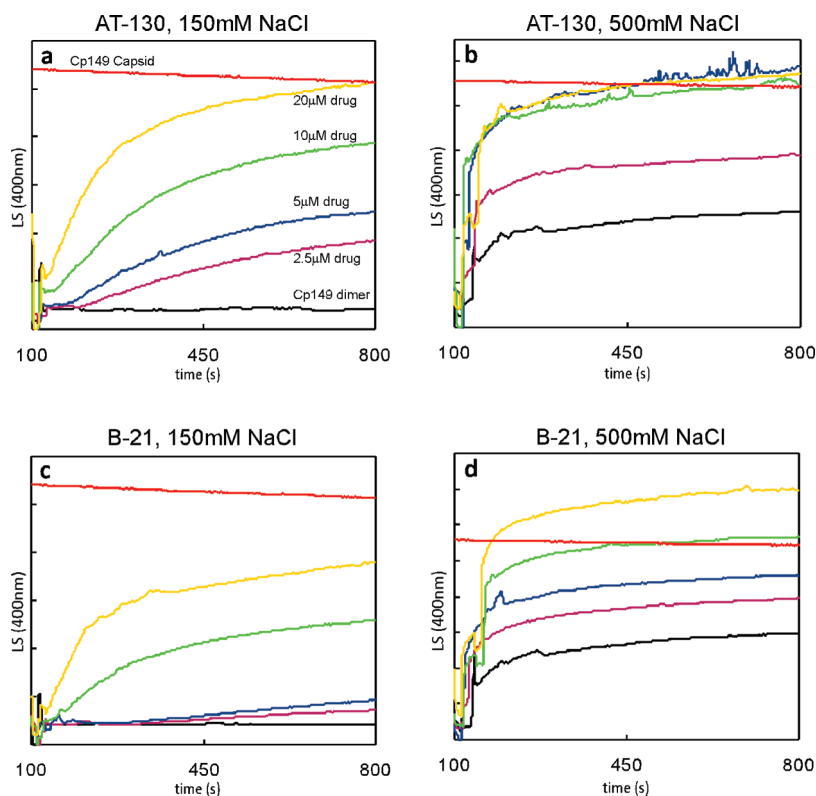
Figure 2. Light scattering traces showing increased rate of 5 μM HBV Cp assembly reactions with phenylpropenamides. a) Cp149 with increasing concentrations of AT-130 with assembly induced with 150 mM NaCl. b) Cp149 with increasing concentrations of AT-130 with assembly induced with 500 mM NaCl. c) Cp149 with increasing concentrations of B-21 with assembly induced with 150 mM NaCl. d) Cp149 with increasing concentrations of B-21 with assembly induced with 500 mM NaCl. The color coding used in panel a applies to all panels.

ments designed to yield approximately 25% assembly. The effect of AT130 in this assay was nearly the same as that of HAP1 (22, 31). B-21 appeared to have a slightly stronger overall effect (data not shown).

To rigorously investigate the effects of phenylpropenamides on assembly in real time, we monitored assembly reactions by light scattering (LS), which is extremely sensitive to the weight-average molecular weight of the solute. The 149-residue assembly domain of the 183-residue HBV core protein (Cp149), which lacks RNA binding activity but assembles into morphologically normal cores, was used for these studies (22, 23). Assembly was initiated by increasing ionic strength. Physiological ionic strength (*i.e.*, 150 mM) results in weak assembly; higher ionic strength results in more aggressive assembly, allowing comparison to previously published standards (10, 23). At 150 mM NaCl, 5 μM Cp149 does not visibly assemble over the course of 800 s (Figure 2), though capsids are evident at 24 h. However, under these conditions, both AT-130 and B-21 increased the rate and extent of Cp149 assembly in a dose-dependent manner (Figure 2).

In the case of AT-130, both the rate of change and overall signal of LS increased with phenylpropenamide concentration until, at a concentration of 20 μM (a 4:1 molar ratio of AT-130 to Cp dimer), assembly reactions reached a maximum at approximately the same LS signal as purified Cp149 capsid (Figure 2, panel a). To look for effects of AT-130-driven assembly under a range of

ate species at high phenylpropenamide concentration. Trapped intermediates appear to be on-path and thus provide a window into the complex assembly reaction of a 120-subunit HBV capsid. These compounds serve as a chemical means to alter the reaction timing, illustrating the importance of the kinetic pathway in successful virus assembly.

RESULTS AND DISCUSSION

Phenylpropenamides Drive Assembly of HBV Capsids. The phenylpropenamide molecules AT-130 and B-21 (Figure 1) were initially tested for assembly activity in a high-throughput screening assay designed to identify HBV capsid assembly effectors (31, 32). Both compounds accelerated HBV core protein assembly and increased its overall extent compared to control experi-

conditions, LS of compound titrations was monitored for 300 mM NaCl (data not shown) and 500 mM NaCl (Figure 2, panel b). A dose-dependent increase in signal was apparent at all salt concentrations, suggesting at least an additive effect. However, rather than the dramatic increase in LS due to aberrant assembly that is observed for the HAP molecules, AT-130 resulted in the same maximal light scattering under all tested conditions. This suggests that assembly proceeds down normal pathways to produce capsids.

Compound B-21 had a similar dose-dependent increase in rate and apparent extent of assembly at low salt concentrations, but the rate and extent of increase of LS was substantially less than that of AT-130 at the same conditions, a trend that continued in the 300 mM NaCl assembly experiments (not shown). However, at 500 mM NaCl the effect was noticeably different. At higher concentrations of B-21, the LS signal reproducibly exceeded that of pure capsid, indicating that B-21 and AT-130 produce different assembly products (Figure 2, panel d).

From these data it is clear that phenylpropenamides are assembly effectors, but they do not behave like HAPs. Comparison of these preliminary studies to HAP-induced assembly raised three points of interest for further study: the stabilization of assembly, the effect of phenylpropenamides on assembly kinetics, and the limited ability of phenylpropenamides to drive assembly off path (or the ability of HBV to overcome the effects of phenylpropenamide binding to maintain assembly on-path).

To quantify the thermodynamic effect of these compounds on HBV capsid assembly, assembly reactions were incubated for 24 h to allow the reactions to approach equilibrium and quantified by size-exclusion chromatography (SEC). Figure 3 shows typical chromatographs for phenylpropenamide titration assembly reactions, with capsid eluting about 0.5 mL after the void volume and dimer emerging about 3 mL before the end of the column. At all salt concentrations (*i.e.*, over a broad range of association energies), AT-130 showed a dose-dependent increase in assembly (Figure 3, panels a−c), even with 2, 3, and 4 mols of phenylpropenamide per mole of HBV dimer. On the basis of the elution profile, AT-130 appeared to drive assembly toward formation of normal assembly products, consistent with the LS data; there was no peak broadening or shifting, which would be expected for trapped intermediates or large aggre-

gates (Figure 3, panels a and b) as has been observed with the HAPs (*22, 23*). Also consistent with the LS experiments, especially at high salt, high phenylpropenamide concentration drove the reaction to 100% assembly of normal capsids. Furthermore, the reaction products of the AT-130 titrations at both high and low salt concentrations, examined by transmission electron microscopy (TEM), were indistinguishable from normal capsids (Figure 4, panels a−c).

In the case of B-21, the SEC chromatographs also showed a dose-dependent increase in assembly of normal capsids and a corresponding depletion of dimer with phenylpropenamide concentration (Figure 3, panels d−f). Consistent with the LS data, B-21 was not as effective as AT-130 (Figure 3, panel d), shifting the equilibrium to a lesser extent for the same conditions. However, at 500 mM NaCl and B-21 concentrations of 15 μM and above, we observed assembly products of intermediate size eluting between capsid and dimer. The amount of protein in this pool increased with B-21 concentration, to the point that there was no longer a distinct dimer peak in the 20 μM assembly reaction, but only capsids and the apparent intermediate species (Figure 3, panel e inset). This is a surprising result; model studies have repeatedly shown that intermediates are not stable compared to free subunit or capsid. Accumulation of assembly intermediates indicates conditions that are strongly deleterious to efficient virion assembly (*18, 33, 34*).

The presence of intermediates in reactions with high concentrations of B-21 suggests that the compound induces strong associations between dimers, leading to kinetically trapped assembly intermediates. These observations were confirmed by TEM images (Figure 4). At 500 mM NaCl and modest concentrations of protein (5 μM) and B-21 (<10 μM), the assembly reactions produced normal capsids (Figure 4, panel d). However, at a 4:1 molar ratio of B-21 to Cp149 dimer assembled in high salt, the assembly products were a heterogeneous mixture of complete and partially formed capsids (Figure 4, panel e). Aggregation and misdirected assembly tends to result in large pleiomorphic polymers with local hexameric symmetry (*12, 22*); in contrast, the micrographs of assembly at this B-21/Cp ratio showed distinct partial and half-spherical particles, indicating that these were in fact intermediates in the assembly of normal capsids. The partial capsids were actually much larger than we expected from their elution by SEC but
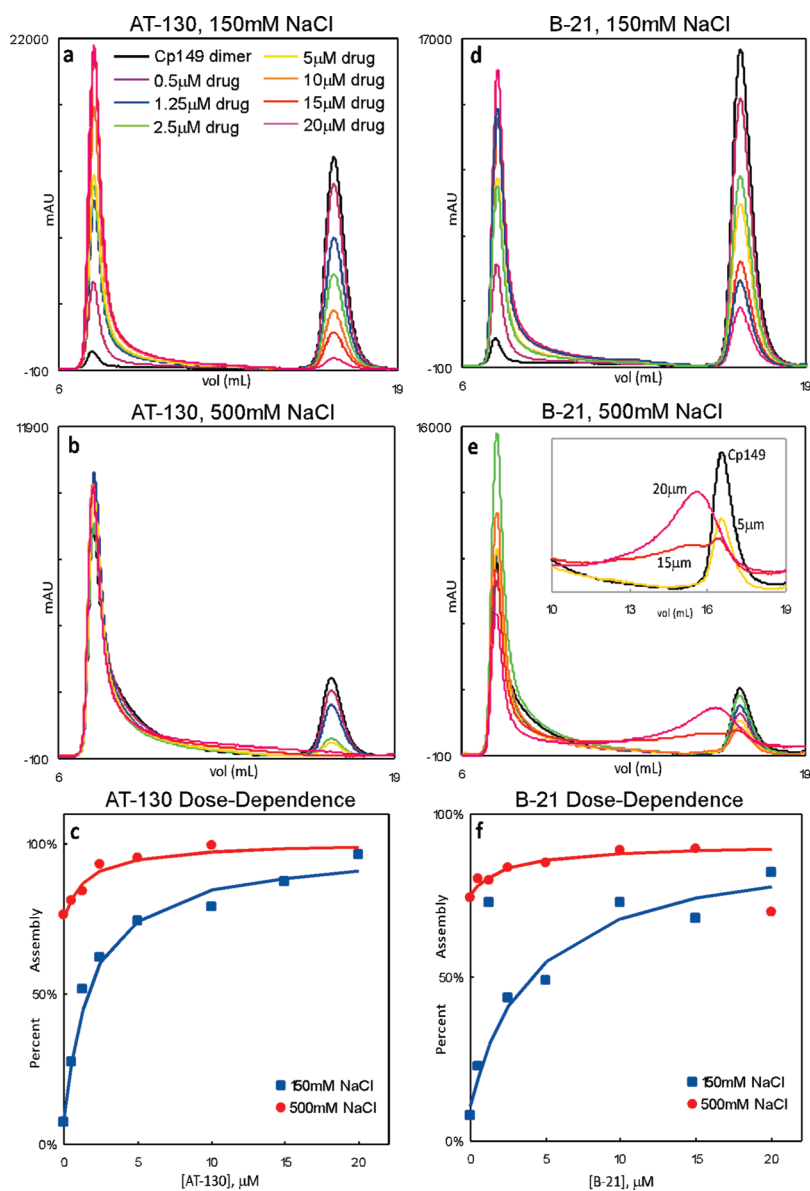
Figure 3. Size exclusion chromatograms of equilibrated 5 μM HBV Cp assembly reactions showing increased assembly with increasing phenylpropenamide concentration. a) Cp149 with increasing concentrations of AT-130 with assembly induced with 150 mM NaCl. **b)** Cp149 with increasing concentrations of AT-130 with assembly induced with 500 mM NaCl. **c)** Cp149 with increasing concentrations of B-21 with assembly induced with 150 mM NaCl. **d)** Cp149 with increasing concentrations of B-21 with assembly induced with 150 mM NaCl. **e)** Cp149 with increasing concentrations of B-21 with assembly induced with 500 mM NaCl. Inset: Expanded view showing intermediate peaks present at 2:1 and 4:1 molar ratio B-21:Cp149 dimer. **f)** Cp149 with increasing concentrations of B-21 with assembly induced with 150 mM NaCl. The color coding used in panel a applies to panels a−d.

were still clearly incomplete and yet unlike any mis-assembled products observed with HAPs. These observations explain the elevated LS signal at high salt and

B-21 concentrations. Virus capsids are large enough compared to the 400 nm light used in the LS experiments that they are not Rayleigh point scatterers (diam-
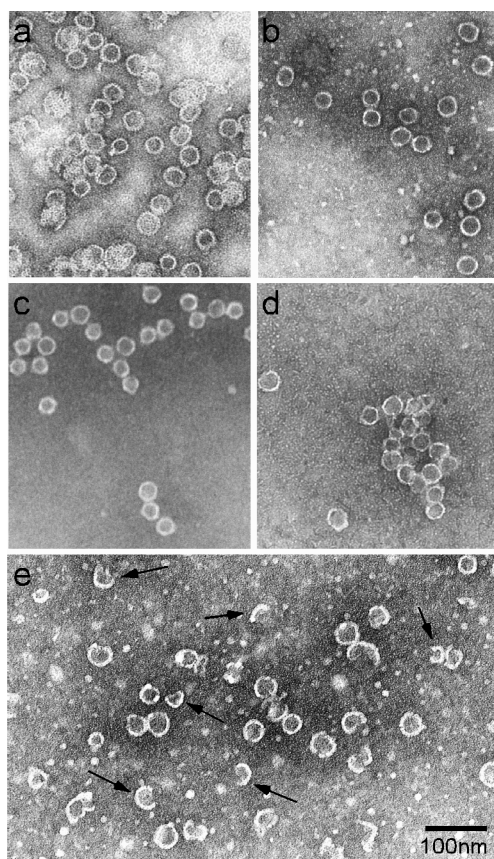
Figure 4. Electron micrographs of HBV/phenylpropenamide assemblies. a) Cp149 assembly showing normal capsids. b) Cp149 assembly with a 1:1 molar ratio of AT-130 to Cp149 dimer. c) Cp149 assembly with 4:1 molar ratio of AT-130 to Cp149 dimer. d) Cp149 assembly with a 1:1 molar ratio of B-21 to Cp149 dimer. e) Cp149 assembly with a 4:1 molar ratio of B-21 to Cp149 dimer. Arrows indicate incomplete/partial capsids. The scale bar in panel e applies to all micrographs.

the result that a kinetically trapped assembly of large intermediates can scatter more light than a reaction with a smaller number of complete particles. For virus-sized particles, there is destructive interference in the light scattered by a single particle so that the signal at 90° from incident does not correlate directly with molecular weight (*35, 36*); a 120-dimer HBV capsid scatters 30 times as much light as the same weight concentration of dimer (*37*).

Quantifying Thermodynamics and Kinetics of Assembly. From the SEC data, we calculated the effect of the phenylpropenamides on capsid stability, which is reported in terms of an analytical evaluation of the pseudocritical concentration of assembly, K_{10}. From capsid stability we have also calculated the change induced by propenamides to pairwise association energy between subunits, $\Delta\Delta G_{contact}$ (*1*). The effect of phenylpropenamides on kinetics is reported as a kinetic index, k_{index}, the negative log of the acceleration of kinetics, that scales well with $\Delta\Delta G_{contact}$ (*23, 38*).

To demonstrate the effect of phenylpropenamides, we observe that the K_{10} drops from approximately 5 μM in the absence of phenylpropenamides to approximately 1 μM for 5 μM Cp149 dimer assembled in 150 mM NaCl and with 10 μM of either AT-130 or B-21, an equimolar ratio of phenylpropenamide to potential sites (Table 1). The change of the contact energy with phenylpropenamide binding ($\Delta\Delta G_{effector}$) was taken as the difference of the free and effector-associated contact energies (*23*). Without information on the binding site or mechanism, we made a lower estimate of the magnitude of $\Delta\Delta G_{effector}$ by assuming quantitative binding (Table 1). Though ionic strength has a substantial effect on $\Delta\Delta G_{contact}$, there was no significant change in $\Delta\Delta G_{effector}$ at different salt concentrations, indicating that the phenylpropenamide effect on assembly was mechanistically independent of the ionic strength effect on as-

eter >5% of the wavelength) (*35*). Thus, a half capsid will scatter proportionally more light per unit mass, with

TABLE 1. Thermodynamic and kinetic parameters of phenylpropenamides at 37 °C

	K_{10} (μM)			$\Delta\Delta G_{drug}$, per contact (kcal mol⁻¹)			Kinetic index	
	0.15 M NaCl	0.3 M NaCl	0.5 M NaCl	0.15 M NaCl	0.3 M NaCl	0.5 M NaCl	0.15 M NaCl	0.3 M NaCl
Cp149	4.87	1.86	1.00	N/A			N/A	
AT-130	1.21	0.067	0.023	-0.99 ± 0.18	-1.02 ± 0.18	-1.13 ± 0.07	-2.08 ± 0.07	-2.96 ± 0.34
B-21	1.31	0.77	0.42	-0.5 ± 0.13	-0.22 ± 0.09	-0.31 ± 0.12	-1.72 ± 0.34	-3.10 ± 0.42

sembly activation. We observed a roughly linear increase in percent assembly as phenylpropenamide concentration increased, even at ratios of four propenamides per dimer, indicating that binding to capsid was not saturated (Figure 3, panels c and e). In short, the dissociation constant of the phenylpropenamides for capsid is ≥10 μM. Additionally, at the strongest values of $\Delta\Delta G_{effector}$, assembly reactions may be starved for reactants and halt short of true equilibrium (33, 39). Therefore the calculated $\Delta\Delta G_{effector}$ for these compounds is an upper limit but still useful for comparison to earlier experiments at similar concentrations of assembly effector. The true $\Delta\Delta G_{effector}$ may be substantially stronger.

The slopes of the LS traces were used to calculate the ad hoc K_{index} (see Methods) (23). Because the units are arbitrary, standards are required to compare different sets of experiments. The kinetic indices for the assembly reactions at 150 and 300 mM NaCl are shown in Table 1; in the 500 mM NaCl assembly reactions, K_{index} could not be calculated because the LS traces were effectively vertical at their maximum points. As with the thermodynamic calculations, the linear dependence of the rate of change in assembly with increasing phenylpropenamide concentration (Figure 5) indicates that even up to 4:1 molar ratios of phenylpropenamide to Cp dimer, the binding sites are not saturated.

We observe that the phenylpropenamides have similar kinetic and thermodynamic effects on assembly as the weaker members of the HAP family of effector molecules. The critical caveat in these calculations is that we assumed that AT-130 and B-21 bound Cp149 core protein with high affinity when calculating the $\Delta\Delta G_{effector}$ and K_{index}. In contrast, HAP binding to capsids is very tight (23, 38), allowing accurate determination $\Delta\Delta G_{effector}$, though binding to dimer was also still in the linear regimen at concentrations of up to 20 μM (23). Interestingly, the ratio of the kinetic index to the $\Delta\Delta G_{effector}$ is greater for the phenylpropenamides than the HAPs; it seems that phenylpropenamides exert a disproportionately larger effect on rate than the yield of product.

Phenylpropenamides Primarily Alter Reaction Kinetics. The phenylpropenamide assembly effectors increase both the rate and extent of assembly and yet produce normal capsids. We have hypothesized that capsid assembly maintains fidelity by thermodynamic editing: the reversible removal of defects in a growing capsid (10, 40). Given the relatively weak $\Delta\Delta G_{effector}$,
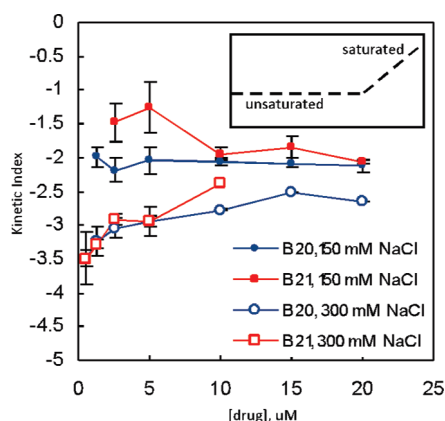

Figure 5. Phenylpropenamide binding does not saturate, even at a 4:1 phenylpropenamide/dimer molar ratio. The kinetic index plotted *versus* increasing drug concentration is approximately constant. The inset shows the behavior expected for the kinetic index when Cp is titrated with assembly accelerator. For these experiments, protein was incubated with AT-130 or B-21 and assembly was induced with 150 and 300 mM NaCl.

we speculated that the phenylpropenamides may be capable of producing large polymers under aggressive assembly conditions, but under conditions tested here, thermodynamic editing prevented their accumulation; the small intermediates observed by SEC at 500 mM NaCl may be shear products. Alternatively, if phenylpropenamides predominantly affect assembly by accelerating nucleation, we should only observe small intermediates that can progress into capsids. To test these competing hypotheses, we turned to sucrose gradient separation of the reaction products, a method less likely to shear fragile polymers like SEC or guide the eye to regular complexes like TEM. Cp149 dimer at 5 μM was assembled with 500 mM NaCl with 4× molar excess AT-130 or B-21 and allowed to equilibrate for 24 h. The reaction components were resolved on a 10%−40% continuous sucrose gradient and fractions quantified by SDS-PAGE.

As previously observed, a reaction containing Cp149 alone assembled into normal capsids, visible in the gradient as distinct populations of $T = 3$ and $T = 4$ particles (fractions 20−25) and unassembled dimer (fractions 35−39), with no apparent intermediates between the capsid bands and the top of the gradient (Figure 6, panel a). When assembled with AT-130, the same two
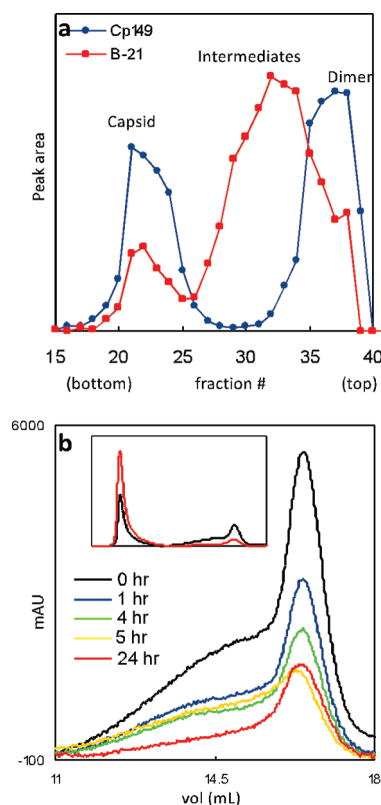
Figure 6. Resolved and persistent kinetic trapping. a) Sucrose gradient quantitation of HBV/phenylpropenamide assemblies. Cp149 (blue) shows only capsid (fractions 20−25) and dimer (fractions 35−39) peaks. Cp149 with a 4× molar excess of B-21 (red) shows a large population of intermediate-sized polymers (fractions 27−35). b) Long-term kinetics of Cp149 with B-21 assembly. Size exclusion traces of Cp149 assembled with equimolar concentrations of B-21 in 300 mM NaCl, sampled by the hour, showing initial accumulation of intermediates that diminishes with time. Inset: Full traces showing all reactants and products.

bands were visible in the sucrose gradient with no visible intermediates (data not shown). However, the sucrose gradient of a B-21 assembly reaction showed that the capsid and free dimer peaks were significantly reduced and that the majority of the protein was trapped in a heterogeneous population of intermediate size (fractions 27−35) (Figure 6, panel a). These data are in agreement with the SEC data showing an intermediate peak (Figure 3, panel e) and consistent with the light scattering data (Figure 2, panel d). From these data it is apparent that B-21 is trapping an array of smaller intermediates, not promoting the assembly of very large fragile aggregates.

To further test for kinetic trapping and thermodynamic editing, we observed the long-term kinetics of assembly with B-21. Cp149 was assembled with an equimolar concentration of B-21 at 300 mM NaCl, conditions where we had previously observed no intermediates at equilibrium (Figure 6, panel b). SEC of this reaction within 5 min after assembly was initiated showed a significant shoulder on the dimer peak. This shoulder elutes at the same position as the intermediate peak observed in the equilibrated assembly with 500 mM salt and 3:1 and 4:1 molar ratios of B-21:Cp dimer (Figure 6, panel b). However, rather than accumulate, this intermediate peak decreased as the reaction progressed until at equilibrium only capsid and dimer were apparent, as seen previously. In the presence of compounds that stabilize protein−protein interactions, random association of HBV capsid protein as a result of off-path assembly should result in relatively stable complexes; in this reaction intermediates either dissociated or were chased into normal, complete capsids, which suggests that these are intermediate species of the normal assembly reaction.

Phenylpropenamides as Probes of the HBV Assembly Pathway. Under aggressive assembly conditions, the phenylpropenamides offer a new view of HBV assembly. The compound B-21 promotes the kinetic trapping that is characteristic of overnucleated assembly, creating many small oligomers that deplete the pool of available subunit for elongation and completion of capsids. This is consistent with the elevated K_{index} and lowered K_{10} in the presence of the phenylpropenamides (Table 1). The decreased pseudocritical concentration (K_{10}) and increased kinetic index indicate that the weak subunit−subunit interactions have been increased to the point that nucleation begins at much lower concentrations of protein and at an increased rate in the presence of the phenylpropenamides. The apparent result is that these intermediates are on-path but kinetically trapped, rather than the structurally altered, off-path reaction products induced by HAPs; EM micrographs support this by showing what appear to be partially formed by otherwise normal capsids, not the large hexamer-rich complexes observed with the HAPs. Pleiomorphic,

noncapsid HAP-induced polymers are aberrant and persist, whereas the phenylpropenamide-induced intermediates are consumed while normal capsids appear, further indicating that the phenylpropenamide-induced traps are steps in the normal assembly process (Figure 7).

As seen in the LS experiments with B-21, the elevated LS signal observed at high salt and excess (2:1 and 4:1 molar ratio) compound indicates that intermediates form early in the assembly reaction. However, that the signal is only modestly increased beyond that of capsid indicates that these are not large, HAP-like, noncapsid polymers. Conditions where there is fast, facile nucleation and strong protein−protein interaction due to high NaCl and $\Delta\Delta G_{effector}$ result in kinetic trapping. As expected, these extreme assembly conditions support persistence of the kinetic traps that would be transient under more gentle conditions (15, 41). We have subsequently shown that at lower effector concentrations and less aggressive assembly conditions, the addition of B-21 does cause kinetic trapping; however, under these milder conditions, the kinetic traps resolve with time to form morphologically normal cores (Figure 6, panel b).

That phenylpropenamide binding causes some conformational change to free dimer is evident by their assembly activating properties, but the formation of normal cores implies that this change appears to be in the realm of normal HBV core protein allostery (20, 24). HAP-1 binding results in minimal tertiary structural changes but affects a global quaternary structural change in the capsid, providing a structural basis for the flat, noncapsid, hexamer-rich polymers observed by TEM (22, 24). In contrast, even the highest concentrations of phenylpropenamides do not divert assembly from the usual assembly products; rather they simply increase the reaction rate and decrease the pseudocritical concentration while still allowing normal quaternary interactions. It is also possible that the phenylpropenamides bias the assembly pathways to decrease the diversity of intermediate species and increase the likelihood of trapping. In either case, phenylpropenamides have provided an experimental access to on-path intermediates for assembly of HBV capsids that may be used to elucidate the individual steps of the core assembly pathway.

The *in vitro* effects of the phenylpropenamide molecules provide a rationale for their observed effects in cell culture. AT-130 decreases viral replication in HepG2 cells with an IC_{50} of 2.5 μM (29). To the authors of that
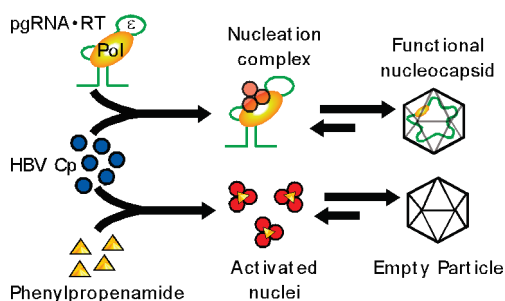

Figure 7. Model of effect of propenamide binding on assembly. Normal HBV assembly is nucleated by the reverse transcriptase−genome complex. The phenyl-propenamides allow for the initiation of capsid assembly by the rapid formation of nuclei without the RT−genome complex, resulting in the formation of empty particles.

study, AT-130 appeared to block viral RNA packaging without interfering in viral protein or RNA synthesis, resulting in the production of empty yet morphologically normal cores (30). The data presented here suggest that the phenylpropenamides are not directly interfering with genome packaging but instead have disrupted the timing of the assembly reaction. Rather than normal assembly initiation by a viral signal or host partner, the phenylpropenamides caused indiscriminate nucleation independent of normal packaging contents, leaving the core protein pool depleted by the rapid and unregulated formation of empty cores. In support of this alternative interpretation, we have noted a linear correlation between the K_{index} of HAP molecules and their EC_{50} in cell culture (23); increased K_{index} decreases the EC_{50}. The K_{index} and the previously determined IC_{50} of AT-130 places it along this trend.

Thus, the phenylpropenamides seem to represent a subclass of assembly accelerators; they do not misdirect assembly, they simply speed it up. The capsid assembly reaction itself proceeds normally, but the delicately timed assembly pathway has been upset. Molecules such as the HAPs, which alter reaction rate and misdirect assembly *in vitro*, may also deplete the pool of free subunits by creating abortive, noncapsid structures and clearing the core protein pool *via* the proteosome (38). Ultimately they bring about the same end result as assembly-accelerating compounds, blocking the normal genome encapsidation process, but the phenylpropenamide compounds seem to achieve this end exclusively by changing the reaction kinetics.

We suggest that even molecules that simply accelerate normal assembly are able to effectively block virus production. *In vitro* we have shown that kinetic effects are obvious even at substoichiometric concentrations. This result is consistent with the presence of a rate-limiting nucleation step in the reaction and that altering this relationship of slow nucleation followed by rapid elongation is devastating to virus assembly (*9*). Molecules that inhibit assembly are likely to be self-limiting in that bound subunits will simply be thermodynamically edited out of the "inhibited" intermediate, or alternatively, inhibited reactions may be overwhelmed by increased production of capsid protein (*40*). In contrast to assembly inhibitors, the effect of assembly accelerators is only enhanced at higher protein concentrations. Thus assembly effectors such as the HAPs and, as we have shown, the phenylepropenamides, that enhance assembly with the binding of only the relatively few molecules necessary to accelerate nucleation are likely to represent a successful assembly directed antiviral strategy.

In conclusion, we have identified the phenylpropenamide family of compounds as a class of assembly effectors of HBV that specifically accelerate normal, on-path assembly. Their effects on assembly have provided insight into the importance of kinetics and assembly pathway of the HBV capsid assembly. Phenylpropenamides have provided a means to trap and study on-path intermediates in the assembly reaction. By comparison to results from cell culture, our results illustrate the importance of timing of assembly in the virus lifecycle (*28, 29*). The identification of the mechanism of phenylpropenamide action as targeting a distinctive viral process provides a unique means for studying the mechanics of virus capsid assembly.

METHODS

Sample Preparation. Cp149 was expressed in *E. coli* from a pET11-based plasmid, pCp149, and purified using the detailed protocol described previously (*42, 43*). Frozen aliquots were dialyzed against an assembly buffer of 50 mM Hepes (pH 7.5) prior to use. Phenylpropenamides were stored at −20 °C as 10 mM stocks in dimethyl sulfoxide (DMSO), which were diluted with the assembly reaction buffer as needed.

Propenamide Synthesis. Compounds AT-130 and B-21 were synthesized following a previously reported procedure (*28*) as shown in Figure 1. Condensation of appropriate benzaldehydes with 4-nitrohippuric acid (**1**) in the presence of sodium acetate in acetic anhydride at 100 °C provided the oxazalone intermediates (**2**), which were ring-opened with piperdine and subsequently brominated. Representative procedures and characterization data are as follows.

*(Z)-4-(2-Methoxybenzylidene)-2-(4-nitrophenyl) Oxazol-5(4H)-one (**2a**).* 4-Nitrohippuric acid (**1**, 0.5 g, 2.23 mmol), *o*-anisaldehyde (0.276 g, 2.23 mmol), sodium acetate (0.183 g, 2.23 mmol), and acetic anhydride (0.6 mL) were combined and heated on a hot plate until the mixture just began to boil. It was then transferred to an oil bath and heated just below the boiling point for 1 h. Hot ethanol (2 mL) was added, and the mixture was stirred until homogeneous and was then cooled to RT. The resulting solid was collected by suction filtration, washed with a minimum quantity of cold ethanol and then with boiling water (approximately 1 mL), and dried *in vacuo* to give **2a** (0.340 g, 68%).

(E)-N-(1-Bromo-1-(2-methoxyphenyl)-3-oxo-3-(piperidin-1-yl)prop-1-en-2-yl)-4-nitrobenzamide (AT-130). To a solution of oxazolone **2a** (0.5 g, 1.54 mmol) in chloroform at 0 °C was added dropwise a solution of piperidine (0.129 g, 1.54 mmol) in chloroform (1 mL). The yellow solution was stirred at 0 °C for 1 h. Solid calcium carbonate (0.154 g, 1.54 mmol) was added, followed by dropwise addition of bromine (0.246 g, 1.54 mmol) in chloroform (2 mL). The suspension was filtered to remove calcium salts, and the resulting solution was evaporated to dryness. The resulting orange oil was recrystallized from ethanol/water (4:1) to give compound AT-130 (0.312 g, 67%) as a colorless powder. ^{1}H NMR

(CDCl₃): δ 0.53−1.44 (m, 4H), 3.30−3.35 (m, 4H), 7.75 (br, 1H, NH), 6.91−7.37 (m, 4H), 7.86−8.44 (m, 4H).

(E)-N-(1-Bromo-1-(2-fluorophenyl)-3-oxo-3-(piperidin-1-yl)prop-1-en-2-yl)-4-nitrobenzamide (B-21). Prepared by the analogous procedure starting with 2-fluorobenzaldehyde. The final compound was isolated as a colorless powder in 70% yield. ^{1}H NMR (CDCl₃): δ 0.53−1.44 (m, 4H), 3.30−3.35 (m, 4H), 7.75 (br, 1H, NH), 7.11−7.39 (m, 4H), 7.97−8.45 (m, 4H).

Light Scattering (LS). Observation of kinetics by light scattering was performed as previously described (*22*). Briefly, scattering was observed with a Photon Technology International fluorometer set for 400 nm for both excitation and emission; 400 nm was chosen as the shortest wavelength for which no reaction component absorbs light. Light scattering was measured for 5 μM Cp149 in 150, 300, and 500 mM NaCl and for phenylpropenamide concentrations of 0.5, 1.25, 2.5, 5, 10, 15, and 20 μM. All measurements were made at 37 °C and using a black masked microcuvette with a 0.3 cm path length (Hellma). Scattering was initially observed for a sample containing approximately twice the final protein concentration in buffer containing no phenylpropenamide or NaCl. After *ca.* 50 s, phenylpropenamide was mixed with the sample so that phenylpropenamide and protein were at twice their final concentrations. After a second observation period of *ca.* 50 s, an equal volume of buffer with twice the final NaCl concentration was added. Light scattering is reported in arbitrary units. All experiments were repeated three times with the exception of the 0.5 and 1.25 μM phenylpropenamide experiments, which were only performed twice at 300 and 500 mM NaCl. After LS experiments, samples were incubated at 37 °C for 24 h for size exclusion experiments.

Size Exclusion Chromatography (SEC). After conducting LS experiments, samples were incubated for 24 h to allow the reactions to approach equilibrium. Previous studies have shown that there is no significant increase in product concentration of Cp149 assembly reactions with longer incubation times; similar experiments have shown that assembly reactions in the presence of the phenylpropenamides reach steady state in approximately half that time. SEC for long-term kinetic and equilibrium experiments was performed using a 21 mL Superose-6 column

equilibrated with 50 mM HEPES pH 7.5 and 0.15 M NaCl. The column was mounted on a Shimadzu-HPLC system equipped with a temperature-controlled autoinjector to facilitate the long time courses and many samples. Equilibrated samples from light scattering experiments were quantified to determine the concentrations of reaction products after 24 h; Cp149 alone shows no further increase in product concentration beyond 24 h, and assembly reactions in the presence of the phenylpropenamides reached a constant concentration of capsid in less than half that incubation period (*25*). Long-term kinetic experiments were performed by sampling a single reaction mix at every hour and separating reactants and products as described.

Calculation of Kinetic and Thermodynamic Parameters. SEC chromatographs at 280 nm were quantified after manual baseline correction using the supplied LCSolutions software for the quantification of reactants and products (Shimadzu). The concentrations of assembled capsid and free dimer subunit were used to determine the apparent dissociation constant and the pairwise contact energies between subunits as described previously (*10*). Briefly, capsid assembly was considered an equilibrium reaction of 120 dimers assembling into a single capsid, from which the equilibrium constant K_{capsid} can be expressed as

$$K_{capsid} = [\text{capsid}]/[\text{dimer}]^{120} \qquad (1)$$

Given the capsid geometry, wherein 120 tetravalent subunits form 240 pairwise contacts, a statistical term that describes this degeneracy can be used to derive the bimolecular $K_{contact}$ as follows:

$$K_{capsid} = \Pi_j s_j (K_{contact})^{240} \qquad (2)$$

where $\Pi_j s_j$ for a 120 subunit $T = 4$ HBV capsid is $2^{119}/120$. From this value, the pairwise contact energies for assembly under a given set of conditions can be determined by

$$\Delta G_{contact} = -RT \ln(K_{contact}) \qquad (3)$$

where R is the gas constant and T is temperature in degrees Kelvin.

An additional useful value, K_D, can be determined from K_{capsid}. $K_{D,app}$ is the apparent dissociation constant, where concentrations of dimer and capsid are equal. $K_{D,app}$ is thus determined by the following:

$$K_{capsid} = K_{D,app}/K_{D,app}^{120} = K_{D,app}^{199} \qquad (4)$$

Capsid assembly can be modeled as a variation of classical polymer theory (*44*). As assembly depends on the interactions of many subunits, below a pseudocritical concentration of subunit, capsids will not form. However, the concentration of free subunit varies with total subunit concentration and is thus an inconvenient value for assembly reaction comparisons. We had previously used the apparent dissociation constant, $K_{D,app}$ (eq 4) as an index of assembly stability. Unfortunately, $K_{D,app}$ occurs at the point where free subunit concentration just begins to plateau and capsids just begin to appear, making the molar quantities difficult to determine. For this reason we now define a new index, K_{10}, that is approximately equal to the experimentally observable pseudocritical concentration of free subunit and is readily calculable. Formally, K_{10} is the concentration of free subunit when the equilibrated concentration of assembled capsid is at high excess compared to $K_{D,app}$, arbitrarily defined here as 10 times $K_{D,app}$:

$$K_{capsid} = 10K_{D,app}/K_{10}^{120} \qquad (5a)$$

$$K_{10} = \exp\{[120(\ln K_{capsid})/119 - 10]/120\} \qquad (5b)$$

The influence of effectors on capsid assembly can be quantified from the change in capsid stability. The average change of subunit contact energy in the presence of the phenylpropenamides can be converted to a weighted average of the contact energies of free and compound-bound Cp dimers:

$$\Delta G_{contact,av} = (1 - \chi_{bound})\Delta G_{contact,free} + \\ \chi_{bound}\Delta G_{contact,bound} \qquad (6)$$

where χ_{bound} is the fraction of subunits bound to the assembly effector (*23*).

Kinetic parameters were derived from light scattering traces. Early time points were visually inspected to determine the region of greatest quantifiable slope. A linear regression of these points provided a numerical value for this maximum slope that was used in subsequent calculations of kinetic index (eq 3), a dimensionless number relating the observed reaction rate to effector concentration. This was calculated as

$$K_{index} = \log(\text{slope}_{max}/[\text{assembly effector}]) \qquad (7)$$

where slope_{max} is the maximum slope of the LS trace in arbitrary units for a given reaction, and [assembly effector] is the micromolar concentration of compound tested in the reaction.

Electron Microscopy. Samples from light scattering experiments were adsorbed to glow-discharged carbon over paralodian copper grids (EM Sciences). Samples were negatively stained with 2% uranyl acetate and visualized with a JEOL 1010 transmission electron microscope equipped with a 4Kx4K Gatan CCD camera.

Sucrose Gradients. HBV assembly reactions of 5 μM Cp149 with or without 20 mM B-21 were assembled with 0.5 M NaCl and allowed to equilibrate for 24 h at 37 °C. Samples were then loaded on a 10−40% (w/v) continuous SW40 sucrose gradient and centrifuged at 150,000 × g at 19 °C for 4 h (*43*). Gradients were harvested from the bottom into ~300 μL fractions. Samples were run on SDS-PAGE gels and silver stained; band intensity was quantified using ImageJ (*45*).

REFERENCES

1. Katen, S., and Zlotnick, A. (2009) The thermodynamics of virus capsid assembly, *Methods Enzymol. 455*, 395–417.
2. Ganem, D., Schneider, R. J. (2001) *Hepadnaviridae: The Viruses and Their Replication*, 4th ed., Lippincott Williams & Wilkins, Philadelphia.
3. Ganem, D., and Prince, A. M. (2004) Hepatitis B virus infection−natural history and clinical consequences, *N. Engl. J. Med. 350*, 1118−1129.
4. Seeger, C., and Mason, W. S. (2000) Hepatitis B virus biology, *Microbiol. Mol. Biol. Rev. 64*, 51−68.
5. Yeh, C. T., Liaw, Y. F., and Ou, J. H. (1990) The arginine-rich domain of hepatitis B virus precore and core proteins contains a signal for nuclear transport, *J. Virol. 64*, 6141−6147.
6. Lan, Y. T., Li, J., Liao, W., and Ou, J. (1999) Roles of the three major phosphorylation sites of hepatitis B virus core protein in viral replication, *Virology 259*, 342−348.
7. Kann, M., Sodeik, B., Vlachou, A., Gerlich, W. H., and Helenius, A. (1999) Phosphorylation-dependent binding of hepatitis B virus core particles to the nuclear pore complex, *J. Cell Biol. 145*, 45−55.
8. Caspar, D. L. D., and Klug, A. (1962) Physical principles in the construction of regular viruses, *Cold Spring Harbor Symp. Quant. Biol. 27*, 1−24.

9. Zlotnick, A. (1994) To build a virus capsid. An equilibrium model of the self assembly of polyhedral protein complexes, *J. Mol. Biol. 241*, 59–67.

10. Ceres, P., and Zlotnick, A. (2002) Weak protein-protein interactions are sufficient to drive assembly of hepatitis B virus capsids, *Biochemistry 41*, 11525–11531.

11. Zhang, T., and Schwartz, R. (2006) Simulation study of the contribution of oligomer/oligomer binding to capsid assembly kinetics, *Biophys. J. 90*, 57–64.

12. Stray, S. J., Ceres, P., and Zlotnick, A. (2004) Zinc ions trigger conformational change and oligomerization of hepatitis B virus capsid protein, *Biochemistry 43*, 9989–9998.

13. Hagan, M. F., and Chandler, D. (2006) Dynamic pathways for viral capsid assembly, *Biophys. J. 91*, 42–54.

14. Rossmann, M. G. (1984) Constraints on the assembly of spherical virus particles, *Virology 36*, 1–11.

15. Schwartz, R., Shor, P. W., Prevelige, P. E. J., and Berger, B. (1998) Local rules simulation of the kinetics of virus capsid self-assembly, *Biophys. J. 75*, 2626–2636.

16. Dykeman, E. C., Stockley, P. G., and Twarock, R. (2010) Dynamic alloetery controls coat protein conformer switching during MS2 phage assembly, *J. Mol. Biol. 395*, 916–923.

17. Twarock, R. (2004) A tiling approach to virus capsid assembly explaining a structural puzzle in virology, *J. Theor. Biol. 226*, 477–482.

18. Zlotnick, A., Johnson, J. M., Wingfield, P. W., Stahl, S. J., and Endres, D. (1999) A theoretical model successfully identifies features of hepatitis B virus capsid assembly, *Biochemistry 38*, 14644–14652.

19. Porterfield, J., Dhason, M. S., Loeb, D. D., Nassal, M, Stray, S. J., and Zlotnick, A. (2010) Full-length hepatitis B virus core protein packages viral and heterologus RNA with similarly high levels of cooperativity, *J. Virol. 84*, 7174–7184.

20. Packianathan, C., Katen, S. P., 3rd., and Zlotnick, A. (2010) Conformational changes in the hepatitis B virus core protein are consistent with a role for allostery in virus assembly, *J. Virol. 84*, 1607–1615.

21. Freund, S. M. V., Johnson, C. M., Jaulent, A. M., and Ferguson, N. (2008) Moving towards high-resolution descriptions of the molecular interactions and structural rearrangements of the human hepatitis B core protein, *J. Mol. Biol. 384*, 1301–1313.

22. Stray, S. J., Bourne, C. R., Punna, S., Lewis, W. G., Finn, M. G., and Zlotnick, A. (2005) A heteroaryldihydropyrimidine activates and can misdirect hepatitis B virus capsid assembly, *Proc. Natl. Acad. Sci. U.S.A. 102*, 8138–8143.

23. Bourne, C. R., Lee, S., Venkataiah, B., Lee, A., Korba, B., Finn, M. G., and Zlotnick, A. (2008) Small-molecule effectors of hepatitis B virus capsid assembly give insight into virus life cycle, *J. Virol. 82*, 10262–10270.

24. Bourne, C., Finn, M. G., and Zlotnick, A. (2006) Global structural changes in hepatitis B capsids induced by the assembly effector HAP1, *J. Virol. 80*, 11055–11061.

25. Zlotnick, A., Ceres, P., Singh, S., and Johnson, J. M. (2002) A small molecule inhibits and misdirects assembly of hepatitis B virus capsids, *J. Virol. 76*, 4848–4854.

26. Stray, S. J., and Zlotnick, A. (2006) BAY 41-4109 has multiple effects on hepatitis B virus capsid assembly, *J. Mol. Recognit. 19*, 542–548.

27. King, R. W., Ladner, S. K., Miller, T. J., Zaifert, K., Perni, R. B., Conway, S. C., and Otto, M. J. (1998) Inhibition of human hepatitis B virus replication by AT-61, a phenylpropenamide derivative, alone and in combination with (−)bea-L-2′,3′-dideoxy-3′-thiacytidine, *Antimicrob. Agents Chemother. 42*, 3179–3186.

28. Perni, R. B., Conway, S. C., Ladner, S. K., Zaifert, K., Otto, M. J., and King, R. W. (2000) Phenylpropenamide derivatives as inhibitors of hepatitis B virus replication, *Bioorg. Med. Chem. Lett. 10*, 2687–2690.

29. Delaney, W. E. t., Edwards, R., Colledge, D., Shaw, T., Furman, P., Painter, G., and Locarnini, S. (2002) Phenylpropenamide derivatives AT-61 and AT-130 inhibit replication of wild-type and lamivudine-resistant strains of hepatitis B virus in vitro, *Antimicrob. Agents Chemother. 46*, 3057–3060.

30. Feld, J. J., Colledge, C., Sozzi, V., Edwards, R., Littlejohn, M., and Locarnini, S. A. (2007) The phenylpropenamide derivative AT-130 blocks HBV replication at the level of viral RNA packaging, *Antiviral Res. 76*, 168–177.

31. Stray, S. J., Johnson, J. M., Kopek, B. G., and Zlotnick, A. (2006) An in vitro fluorescence screen to identify antivirals that disrupt hepatitis B virus capsid assembly, *Nat. Biotechnol. 24*, 358–362.

32. Zlotnick, A., Lee, A., Bourne, C. R., Johnson, J. M., Monanico, P. L., and Stray, S. J. (2007) In vitro screening for molecules that affect virus assembly (and other protein association reactions), *Nat. Protoc. 2*, 490–498.

33. Bruinsma, R. F., Gelbart, W. M., Reguera, D., Rudnick, J., and Zandi, R. (2003) Viral self-assembly as a thermodynamic process, *Phys. Rev. Lett. 90*, 248101.

34. Rapaport, D. C. (2008) Role of reversibility in viral capsid growth: a paradigm self-assembly, *Phys. Rev. Lett. 101*.

35. Tanford, C. (1961) *Physical Chemistry of Macromolecules*, John Wiley and Sons, Inc., Hoboken, NJ.

36. Hahn, D. W. (2004) *Light scattering theory*, Department of Mechanical and Aerospace Engineering, University of Florida.

37. Ceres, P., Stray, S. J., and Zlotnick, A. (2004) Hepatitis B virus capsid assembly is enhanced by naturally occurring mutation F97L, *J. Virol. 78*, 9538–9543.

38. Deres, K., Schroder, C. H., Paessens, A., Goldmann, S., Hacker, H. J., Weber, O., Kramer, T., Niewohner, U., Pleiss, U., Stoltefuss, J., Graef, E., Koletzki, D., Masantschek, R. N., Reimann, A., Jaeger, R., Gross, R., Beckermann, B., Schlemmer, K. H., Haebich, D., and Rubsamen-Waigmann, H. (2003) Inhibition of hepatitis B virus replication by drug-induced depletion of nucleocapsids, *Science 299*, 893–896.

39. Endres, D., and Zlotnick, A. (2002) Model-based analysis of assembly kinetics for virus capsids or other spherical polymers, *Biophys. J. 83*, 1217–1230.

40. Bourne, C., Katen, S. P., Fultz, M. R., Pachianathan, C., and Zlotnick, A. (2009) A mutant hepatitis B virus core protein mimics inhibitors of icosahedral capsid self-assembly, *Biochemistry 48*, 1736–1742.

41. Basnak, G., Morton, V., Rolfsson, Ó., Stonehouse, N. J., Ashcroft, A. E., and Stockley, P. G. (2010) Viral genomic single-steanded RNA directs the pathway toward a T = 3 Capsid, *J. Mol. Biol. 395*, 924–936.

42. Zlotnick, A., Cheng, N., Conway, J. F., Booy, F. P., Steven, A. C., Stahl, S. J., and Wingfield, P. T. (1996) Dimorphism of hepatitis B virus capsids is strongly influenced by the C-terminus of the capsid protein, *Biochemistry 35*, 7412–7421.

43. Zlotnick, A., Palmer, I., Stahl, S. J., Steven, A. C., and Wingfield, P. T. (1999) Separation and crystallization of T = 3 and T = 4 icosahedral complexes of the hepatitis B virus core protein, *Acta Crystallogr., Sect. D: Biol. Crystallogr. 55*, 717–720.

44. Oosawa, F., Asakura, S. (1975) *Thermodynamics of Polymerization of Protein*, Academic Press, London.

45. Rasband, W. S. (1997−2005) *ImageJ, U.S. National Institutes of Health*, Bethseda, MD.